Acoustic-phonon emission due to localized photoexcitation of Si: Electron-hole droplets versus the phonon hot spot

Sergei E. Esipov, Madeleine Msall, and J. P. Wolfe
Department of Physics and Material Research Laboratory, University of Illinois at Urbana-Champaign, 1110 West Green Street, Urbana, Illinois 61801
(Received 23 October 1992)

We consider theoretically the evolution of nonequilibrium carriers and phonons created by optical excitation of Si at low temperatures ($T < 2$ K) in light of recent heat-pulse experiments. At low excitation levels (≤ 20 W/mm^2), the detected phonons indicate a quasidiffusive propagation mode, involving anharmonic decay and elastic scattering of relatively high-frequency (≥ 1 THz) phonons. At intermediate excitation densities (≥ 20 W/mm^2) a transition is observed to a localized source of relatively low-frequency (≤ 1 THz) phonons. The threshold for this effect is much lower than that predicted for the formation of a hot spot involving only the phonon system. We interpret these data in terms of the phonons generated in the presence of electron-hole droplets. It is well known that nonequilibrium carriers emit optical and acoustic phonons in their energy relaxation and recombination. At moderate excitation densities droplets of electron-hole liquid are formed. These droplets modify both relaxation and recombination processes of photoexcited carriers due to the increased carrier-carrier scattering in the dense (3×10^{18} cm^{-3}) liquid. Hot carriers, excited by the initial optical excitation or by Auger recombination in the droplets, transfer their kinetic energy to colder carriers in the droplets, partially bypassing the generation of optical phonons and heating the droplets. Our calculations indicate that this process can provide a mechanism for the production of a localized source of low-frequency phonons, as observed in the heat-pulse experiments.

I. INTRODUCTION

The optical excitation of a semiconductor such as Si produces phonons as a byproduct of electronic relaxation. At low excitation density and temperature most of these phonons diffuse away from the excitation point and down convert to lower frequencies by anharmonic processes. At high optical densities an anomalous localization of the thermal energy occurs, attributed in some work to a phonon hot spot. Recent experiments made by some of us[1] provide an opportunity to revisit the physics of the phonon hot spot in Si. The idea of the hot spot[2,3] describes a stage in nonequilibrium phonon kinetics when the excitation energy is high enough to create high local occupation numbers of hot phonons in the otherwise cold crystal. Initially, the phonon energy relaxation may proceed via spontaneous scattering of each phonon into two daughter phonons, thus increasing the occupation numbers. With a sufficient number of initial high-frequency phonons the occupation numbers can reach unity while the corresponding phonon energy is high and initiate the opposite process of phonon coalescence. Because hot phonons are strongly affected by elastic impurity scattering and thus tend to remain localized in space, an effective "bottleneck" may appear in energy and real space leading to the formation of a hot spot.

Heat-pulse experiments on directly photoexcited Si provide an opportunity to test these ideas.[1,4] Figure 1 shows the signal intensity as a function of time (time trace) for two different excitation levels. These data are taken with a 10-ns Ar^+ laser with a *fixed total energy* per pulse; the power density is varied by changing the size of the excitation area. At low power density (trace 2) a small component of early arriving "ballistic" phonons is followed by a long tail, presumably caused by higher-frequency phonons which diffuse and down convert on their way to the detector. This later behavior is termed "quasidiffusion,"[2,5] and the long tail is shown to be roughly consistent with the known anharmonic decay and elastic-scattering mechanism.[1] At higher power density (trace 1), a large increase in the phonon flux arriving near the ballistic time t_b, is observed, accompanied by a decrease in the signal intensity at late times. Here, ballistic phonons are those with a mean free path due to

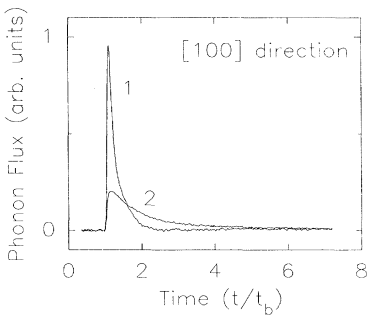

FIG. 1. Experimental time trace showing the detected phonon signal at low (trace 2) and high (trace 1) power density. At high power densities there is a greater proportion of low-frequency phonons which causes an increase in the signal arriving near the ballistic time, $t_b \approx 1$ μs.

scattering from isotopic defects which is greater than the crystal thickness. For a 5.5-mm-thick Si sample this corresponds to phonons with frequencies less than 0.9 THz ($h\nu \leq 3.7$ meV). The observed increase in the ballistic flux at high power density cannot be due to phonon focusing effects because the excitation area is always within a small region around the [100] direction where the ballistic intensity does not change significantly with position. [This fact is verified by using an evaporated metal film (low-frequency) emitter under the same conditions.] The increase in low-frequency phonons reflected in trace 1 can only be due to the onset of a new source of low-frequency phonons at high excitation levels.

Figure 2 plots the intensities of the "peak" phonon signal and the late-time "tail" signal as a function of power density, obtained by changing the excitation area at constant power. The signals for several different incident powers are normalized to the same low-power peak height. There is a clear transition in the character of the heat pulses starting at a surface power density of about 2×10^3 W/cm^2. We interpret this transition as a threshold for the formation of a low-frequency phonon source. In order to compare the experimental power density threshold with the expectations of the hot spot theory[2] we have to estimate several phonon characteristics. In the case of quasidiffusive transport in Si, a phonon is elastically scattered by isotopes with the rate $1/\tau_e = 2.43\times10^{-42}\ \nu^4 s^3$, where ν is the frequency.[6] The third-order anharmonic decay time is $1/\tau_a = 7.41\times10^{-56}\ \nu^5 s^4$.[7] This gives the diffusion length over the phonon lifetime

$$l = (\tfrac{1}{3} s^2 \tau_e \tau_a)^{1/2} = 1.22\times10^{54} \nu^{-9/2}\ \text{cm s}^{-9/2}\ , \qquad (2.1)$$

which can be also rewritten as

$$l(t) = 3\times10^4 t^{9/10}\ \text{cm s}^{-9/10}\ , \qquad (2.2)$$

assuming the mean picture of phonon generations. In Eq. (2.1) s is assumed to be the longitudinal sound velocity. Equation (2.1) predicts that the characteristic frequency of phonons which are able to escape from the $d = 10^{-4}$-cm-thick absorbtion layer is $\nu_d = 8.1$ THz. (We note that this frequency is comparable with the Debye frequency so, for these phonons, the quasidiffusion theory[2] is at best an approximation.) The time for phonons of frequency ν_d to escape the optical excitation region is 0.39 ns, which is shorter than the experimental pulse duration, 10 ns. We deal, therefore, with the so-called prolonged pumping case and following Ref. 2 further, we predict a phonon hot spot threshold,

$$P_0 = \epsilon(\nu_d) d = 8.2\times10^{-4} h \nu_d^4 d\ \text{s}^{-3} = 1.5\times10^{-3}\ \text{J/cm}^2\ ,$$

corresponding to a surface power density $W_0 = P_0/\tau(\nu_d) = 4\times10^6$ W/cm^2. Here, $\epsilon(\nu)$ is the energy density $1.2 h\nu^4/s^3$. The estimate assumes a uniform phonon distribution over the range $0 \leq \nu \leq \nu_d$. The experimental threshold surface power density of 2×10^3 W/cm^2 is *three orders* of magnitude less than this predicted hot spot threshold. Therefore, we conclude that the experimentally observed effect cannot be due to the phonon hot spot envisioned in Ref. 2. Indeed, we believe that the above-mentioned phonon hot spot conditions probably cannot be reached in Si under direct photoexcitation due to the presence of carriers.

Our observations imply that there is a localization of the excitation energy which cannot be explained solely by the dynamics of phonons, as in the hot spot model. This paper offers a possible explanation of the evolution of the excitation energy of a Si sample which includes the essential role of nonequilibrium carriers.

We begin by noting that the measured phonon source lifetime in the experiments[1,4] is 160±30 ns at high excitation levels. This time is comparable with the 140-ns lifetime reported for electron-hole droplets (EHD) in Si.[8,9] It is generally accepted that the nonequilibrium carriers, which have high initial kinetic energies due to the excess optical excitation energy of Auger processes, relax by optical-phonon emission, implying that the main part of carrier cooling proceeds by this process regardless of electron-hole plasma or EHD presence.

In this paper we show that it is unrealistic to ignore the role of the EHD in cooling hot carriers. In Si, the EHD carrier density varies from 10^{18} cm^{-3} at 22 K when the liquid is formed up to 3×10^{18} cm^{-3} at lower temperatures.[8,9] This density is high enough to cause strong *intercarrier* scattering,[10] permitting a hot carrier in the droplet to transfer its excess kinetic energy to the droplet as a whole, rather than emitting optical phonons. Of course there will be a competition between the two processes which depends on the carrier density. If the intercarrier scattering process dominates optical-phonon emission, the droplets may serve as the needed mechanism for low-frequency phonon production. An additional factor is the reabsorption of phonons in the cloud of droplets, which reduces the phonon mean free path.

This paper is organized as follows. In Sec. II we semiquantitatively describe the evolution of carriers and phonons and indicate the possible links between them. We then calculate the intercarrier cooling rate and compare

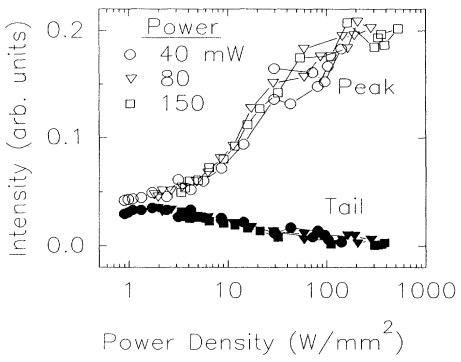

FIG. 2. Peak heights (integrated over $t_b \leq t \leq 1.05 t_b$ in Fig. 1) and tail heights (over $1.2 t_b \leq t \leq 1.6 t_b$) as a function of power density for four different total powers. The data are scaled by the total intensity detected in the heat pulse (integrated over $t_b \leq t \leq \infty$). A transition in the character of the heat pulse occurs at a power density above 20 W/mm^2.

it with the optical-phonon emission in Sec. III. The spectrum of low-frequency phonons emitted by a droplet is calculated in Sec. IV with and without screening effects, showing that the observed low-frequency phonons may indeed be emitted directly by droplets. In Sec. V we test the calculation by estimating the minimum temperature which a droplet may have due to the Auger heating. Comparison with experimental observation suggests that screening effects in EHD are ineffective, as previously assumed by Keldysh and Sibel'din.[11] It also follows that the droplet temperature depends upon the droplet size distribution. Section VI is a summary of our results.

II. EVOLUTION OF CARRIERS AND PHONONS

In this section we semiqualitatively outline the processes which must be considered to understand the spectrum of phonons emitted from a localized photoexcitation of a pure silicon crystal. The carriers and phonons resulting from a cavity-dumped Ar^+ laser pulse of specified character are considered in succession.

A. Carriers

Due to optical excitation with visible light ($h\nu=2.4$ eV), carriers are created high in their bands with excess kinetic energies about $8\hbar\Omega_0$ (holes) and $12\hbar\Omega_0$ (electrons), where $\hbar\Omega_0$ is the optical-phonon energy (see Sec. III). The relaxation due to deformation-potential optical-phonon emission ensures that within 2–3 ps the carriers descend down to the "passive" region ($\epsilon<\hbar\Omega_0$). During this short interval the carrier diffusion in space does not exceed the optical-absorption length $d=10^{-4}$ cm. Intercarrier scattering, however, may accelerate relaxation. Subsequently, the carriers in the passive energy range relax due to deformation-potential acoustic-phonon scattering, so that the relaxation time and the accompanying bipolar diffusion length depend upon the final energy. If one takes the final energy to be close to 5–10 K then the relaxation time is about a nanosecond and the diffusion length is $l_{bd}\approx 10$ μm. This allows us to estimate an average "initial" plasma concentration just following a 10-ns pulse of energy 3×10^{-8} J and focal spot area of 10^{-4} cm^2 to be $n_a\leq 10^{18}$ cm^{-3}, assuming l_{bd} computed above. At lattice temperatures below 22 K this plasma completes the relaxation by forming droplets, while the occupied depth expands to about 50 μm in approximately 20 ns.[12] The average plasma concentration at this time is about 2×10^{17} cm^{-3}. The droplet concentration is estimated to be $n_d=2\times10^{13}$ cm^{-3}, assuming $R=0.1$ μm.[8] Droplets emit low-frequency acoustic phonons (Sec. IV) to cool themselves, and undergo recombination and evaporation. The measured droplet lifetime, $\tau_{\text{Auger}}=140$ ns, is attributed to Auger recombination,[13] whereby an electron and hole recombine by giving a kinetic energy roughly equal to the semiconductor gap (1.1 eV) to one or two remaining carriers. This Auger recombination mechanism presumably heats the droplets somewhat,[10,11,14,15] preventing them from reaching the lattice temperature (see Sec. V).

B. Phonons

Two types of phonons will be emitted in the process of carrier cooling: optical and acoustic. Only carriers in the "active" energy region, $\epsilon>\hbar\Omega_0$, can emit optical phonons, but they can also relax by giving their kinetic energy to a cooler surrounding plasma. (This would seem to be a good possibility for the hot carriers created by Auger recombination in an electron-hole droplet.) One of the principal aims of this paper is to estimate the fraction of excess energy which goes directly into optical phonons. For the moment, let us assume that some number of optical phonons are generated. They down convert to high-frequency acoustic phonons and contribute to the quasidiffusion process.

Ignoring any scattering from carriers, these quasidiffusing phonons occupy at time t the region of the size given by Eq. (2.2), which at 20 ns is comparable to the region occupied by plasma. Using the formula for anharmonic decay, we find that the average phonon frequency at time $t=20$ ns is 3.7 THz. How are these phonons affected by the presence of electron-hole droplets? Short-wavelength acoustic phonons with the momenta larger than twice the Fermi momentum in the liquid cannot be absorbed in the droplet because of conservation principles.[16,17] In particular, for the acoustic phonons with frequencies above $\sqrt{8m_h s^2\epsilon_F}/hs\approx 1.7$ THz the EHD are transparent.[16] Plasmon excitation is also unlikely to occur by short-wavelength phonons.

Based on these considerations, we believe that the main part of the measured "peak" signal (Fig. 1) is due to low-frequency acoustic phonons emitted from the early plasma and droplets. These phonons travel ballistically across the sample and the duration of this pulse indicates the source lifetime. We show in Sec. IV that the calculated emission spectrum for droplets is centered around 0.5 THz, consistent with this interpretation. Theoretically, the energy content of this peak could be up to 50% of the gap energy per pair if the Auger electron relaxation length is about the droplet size, an issue which we consider in Sec. IV. Furthermore, it seems plausible that the emitted optical phonons and their subsequent generations do not interact significantly with EHD. These phonons contribute to the long tail of the time trace in Fig. 1 and would form a phonon hot spot, if there were enough of them. However, simple estimates show that this is not the case under the present excitation conditions, or even excitation levels two orders of magnitude higher.

III. RELAXATION OF HOT CARRIERS IN EHD

We shall disregard initially the finite size of EHD and calculate the competition between intercarrier scattering and optical-phonon emission in a large droplet. All the estimates below are done within the framework of the simple model of isotropic band structure, the constants and notations used are collected in the Appendix. The numerical estimates may be affected by this simplifying approximation, but we believe that the intermediate role

of EHD or dense plasma in controlling the vibrational energy spectrum is fairly represented in the following calculations.

At the onset of laser irradiation the carriers relax independently and accumulate near the bottoms of their bands in a time less than a nanosecond. With a laser pulse duration of 10 ns roughly all the excited carriers relax in the presence of electron-hole plasma or droplets. The droplet temperature is low (although somewhat different from that of the lattice[13]) so the carrier statistics do not play a significant role in hot-carrier relaxation. We are dealing mainly with "dynamic friction."[10,18] The dynamic friction is the rate at which energy is redistributed among the carriers, given by

$$A=-\frac{\hbar\Omega_0}{\tau}\left[\frac{\hbar\Omega_0}{\epsilon}\right]^{1/2}, \tag{4.1}$$

where Ω_0 is the optical-phonon energy, ϵ is the carrier energy, and the $\bar{\tau}$ is the nominal carrier cooling time (see the Appendix or the review[10]). There are three different types of intercarrier collisions going on simultaneously: *ee*, *hh*, and *eh* scattering. Therefore the corresponding energy-loss rates for electrons and holes are the following:

$$\begin{aligned} A_{ec}&=A_{ee}+A_{eh}\ , \\ A_{hc}&=A_{hh}+A_{he}\ . \end{aligned} \tag{4.2}$$

The relaxation of the hot carrier high above the emission threshold $\hbar\Omega_0$ is described as a sequence of emitted phonons with the energy-loss rate,

$$A_O=-\frac{\hbar\Omega_0}{\tau_O(\epsilon)},\quad \frac{1}{\tau_O(\epsilon)}=\frac{1}{\bar{\tau}_O}\left[\frac{\epsilon-\hbar\Omega_0}{\hbar\Omega_0}\right]^{1/2}, \tag{4.3}$$

where we neglect the step-type character of emission, the oscillations connected with it,[10] and the screening effects. The nominal times $\bar{\tau}_O$ for electron and holes are given in the Appendix.

Thus, the total rate of energy loss for electrons and holes are the following:

$$\begin{aligned} \dot{\epsilon}_e&=A_{ee}+A_{eh}+A_{Oe}\ , \\ \dot{\epsilon}_h&=A_{hh}+A_{he}+A_{Oh}\ . \end{aligned} \tag{4.4}$$

The initial conditions are $\epsilon_e(0)=\epsilon_1$ and $\epsilon_h(0)=\epsilon_2$, where the excess energy provided by a photon, $\Delta\epsilon=h\omega-\epsilon_g$, is distributed between the electron and hole in proportion to their masses, i.e., $\epsilon_1=(\Delta\epsilon)m_h/(m_e+m_h)$, $\epsilon_2=(\Delta\epsilon)m_e/(m_e+m_h)$. Using the appropriate parameters for Eqs. (4.1) and (4.3), we compute the time evolution of the electrons and hole kinetic energies and plot the results in Fig. 3(a). The relative strengths of the intercarrier (*ec* and *hc*) and carrier-phonon [deformation-potential optical-phonon (DO)] processes are shown. The intercarrier scattering dominates the relaxation at this density (3×10^{18} cm^{-3}). Note that according to Eqs. (4.1) and (4.3) the intercarrier relaxation speeds up as time goes by, while the optical-phonon emission slows down. In about 0.3 ps the *e-h* pair is already in the passive region with energy $\epsilon<\hbar\Omega_0$. The solution for a lower concentration, $n=10^{18}$ cm^{-3}, is shown for comparison in Fig. 3(b). Lower carrier density slows the intercarrier scattering processes and the direct emission of optical phonons becomes more important, although still secondary.

We now calculate the portion of the initial energy per *e-h* pair which is transmitted to EHD, Q_{cc}. Integrating $A_{ec}+A_{hc}$ over time and using Eqs. (4.4) to change the variables, we have

$$Q_{cc}=\int_{\hbar\Omega_0}^{\epsilon_1}\frac{d\epsilon}{1+A_{Oe}/A_{ec}}+\int_{\hbar\Omega_0}^{\epsilon_2}\frac{d\epsilon}{1+A_{Oh}/A_{hc}}\ . \tag{4.5}$$

The fraction of initial excess energy given to other carriers in the droplet, namely $Q_{cc}/(\Delta\epsilon-\hbar\Omega_0)$, is shown as a

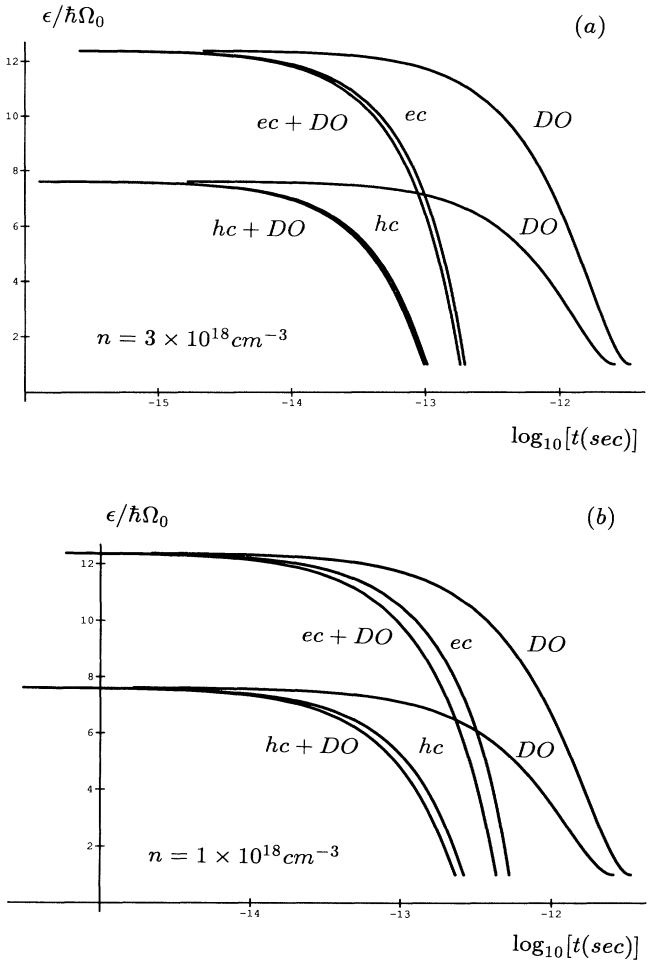

FIG. 3. Time-dependent energy relaxation of hot electrons and holes. The initial energy of $20\hbar\Omega_0$ is distributed between electron and hole so that the initial energy of an electron is $\epsilon_1=12.38\hbar\Omega_0$, and that of a hole is $\epsilon_2=7.62\hbar\Omega_0$, as discussed in the text. Curves show relaxation for DO scattering (deformation potential, optical phonon), cc scattering (carrier-carrier), and DO-cc scattering combined separately for electrons and holes. Carrier concentrations are (a) 3×10^{18} cm^{-3} and (b) 10^{18} cm^{-3}.

function of excitation energy and plasma concentration in Fig. 4. Approximately 90% of the initial energy is directly transmitted to EHD at $n=3\times10^{18}$ cm^{-3}, the equilibrium density of EHD at $T=0$. If we recall that screening (which affects mainly the phonon emission) was not taken into account, we conclude that optical-phonon emission is negligible in a droplet. The situation may change considerably if we study a small droplet, and droplets in Si are believed to be small, $R\approx0.1$ μm.

The role of the droplet in hot-carrier cooling begins in the initial stage just after photon absorption, once the density of previously excited carriers is large, and continues at later stages, when carriers are again excited by Auger recombination. The plasma heating by Auger recombination has been discussed previously in a similar context.[8,10,11,14,15] Rice *et al.* argued that the energy relaxation of Auger excited carriers may occur outside of the droplets,[8] because the relaxation length exceeds the droplet size. This estimate assumes *quasiballistic* motion

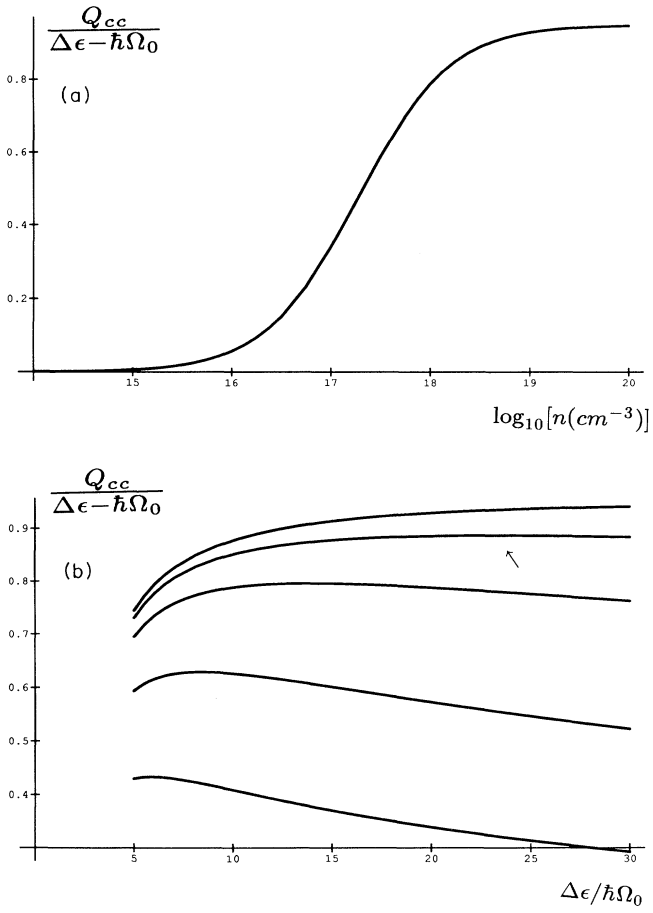

FIG. 4. Fraction of the hot e-h pair energy losses, $Q_{cc}/(\Delta\epsilon-\hbar\Omega_0)$, transmitted to EHD via intercarrier scattering (a) as a function of carrier concentration, and (b) as a function of the dimensionless total energy $\Delta\epsilon/\hbar\Omega_0$. (b) contains a family of curves for different concentrations: $n=0.1$, 0.3, 1.0, 3.0, 10.0×10^{18} cm^{-3} from bottom to top. The curve for $n=3\times10^{18}$ cm^{-3} in indicated by an arrow.

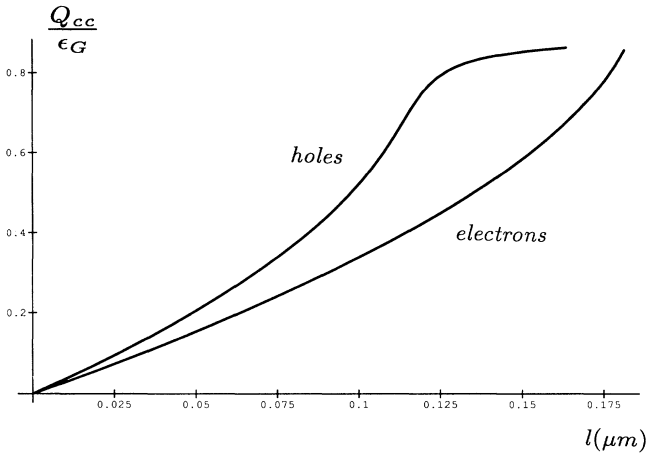

FIG. 5. Fraction of the excess energy retained by a hot carrier in the droplet as a function of the carrier path length l inside the droplet. The initial carrier energy is the gap width. The upper curve is for holes and the lower is for electrons. At present the relative input of these two channels of Auger recombination is unknown. Note that for the path length 0.2 μm the entire hot-carrier excess energy is retained in the droplet, rather than being emitted by optical phonons.

of the hot carrier with a large velocity, 10^8 cm/s, so that it takes only $\sim10^{-13}$ s to leave the droplet. However, the scattering time due to intercarrier scattering is short and, as seen in Fig. 3(a), relaxation is nearly complete in 10^{-13} s. So, we have a delicate situation which requires additional calculations.

The mean straight path to leave a sphere of radius R from arbitrary point inside is $0.76R$. This path is short enough that the amount of energy loss can be simply estimated as $(0.76R/v)A$ where v is the velocity of the hot carrier and A is the loss rate given by Eq. (4.2). Figure 5 shows the fraction of excess hot-carrier energy transmitted to the droplet as a function of the hot-carrier pathlength, l, inside the droplet. Ignoring the fact that energy loss has a nonlinear path dependence, we conclude that approximately 50% of the kinetic energy of an excited carrier would be transferred back to a droplet of 0.1-μm radius. One large-angle scattering event is enough to return all the energy to the parent droplet. It is also possible for an escaped hot carrier to relax inside adjacent droplets, which we do not consider. These results are clearly sensitive to the average droplet size, but we conclude that EHD with 0.1-μm radius or greater are effective in cooling hot carriers by intercarrier scattering, thereby inhibiting the production of high-frequency optical phonons.

IV. SPECTRUM OF EMITTED ACOUSTIC PHONONS

We now calculate the spectrum of phonons emitted by droplets. We follow the usual procedure for the phonon wind.[8,9,11,16] From the first principles we may write the emission rate of acoustic phonons with energy sq via the deformation-potential scattering,

$$W_{ac}(sq)=\left\langle 2\pi|M_q|^2\delta\left[\frac{k^2}{2m_e}-\frac{(\mathbf{k}-\mathbf{q})^2}{2m_e}-sq\right]\times f_e(\epsilon_k)[1-f_e(\epsilon_{\mathbf{k}-\mathbf{q}})](N_q+1)\right\rangle+W_{ac-h}\ , \tag{5.1}$$

where $|M_q|^2=\pi sqS(q)/k_e^3\tau_{Ae}$ is the squared matrix element and the nominal time for acoustic-phonon emission τ_{Ae} is given in the Appendix (see also Ref. 19), f_e is electron distribution function, and N_q is the distribution of the ambient acoustic phonons which is assumed to be a Planck distribution. Averaging in (5.1) is performed over the possible scattering angles and electron energy distribution. The term W_{ac-h} stands for the corresponding expression for holes. The function $S(q)$ describes static screening effects, which we estimate to be

$$S(q)=\left[\frac{\lambda_{\rm TF}^2q^2}{1+\lambda_{\rm TF}^2q^2}\right]^2,$$

where $\lambda_{\rm TF}$ is the Thomas-Fermi screening length. The screening strongly influences the calculations. From energy conservation we find that the possible momenta of emitted phonons satisfy the inequality $q\le 2(k-ms)$ and we rewrite Eq. (5.1) as follows:

$$W_{ac}(sq)=\frac{m_es(N_q+1)}{2\tau_{Ae}k_e^3}S(q)\times\int_{q/2+ms}^{\infty}dk\ kf_e(\epsilon_k)[1-f_e(\epsilon_k-sq)]+W_{ac-h}. \tag{5.2}$$

This spectrum is plotted in Fig. 6 in the presence and absence of screening along with the pure Planck distributions for comparison. We remind that the screened case is not considered relevant (see below). The difference between the unscreened and the Planck spectra comes from the spontaneous emission term and the exclusion principle. The exclusion principle affects mainly large phonon energies when the two Fermi distributions encountered in (5.2) cease to overlap. It is seen from Fig. 6 that the maximum of the energy flux is in 0.5 THz phonons for a droplet temperature of 5 K (see Sec. V). These phonons can account for the measured phonon signal.

Absorption spectra of low-frequency phonons can also be calculated. The absorption length $l_{\rm ab}(\omega)=s\tau_{\rm ab}(\omega)$ is shown in Fig. 7 at different EHD temperatures, with and without screening. The absorption time is

$$\frac{1}{\tau(\omega)}=\frac{m_es}{2\tau_{Ae}k_e^3}S(\omega/s)\times\int_{\omega/2s-ms}^{\infty}dk\ kf_e(\epsilon_k)[1-f_e(\epsilon_k+\omega)]+\frac{1}{\tau_{ac-h}}\ , \tag{5.3}$$

where the last term accounts for holes. Notice that when screening is included the mean free path of the phonons is typically lengthened by one or two orders of magnitude. The large mean free paths computed in the screened case seem inconsistent with the "phonon-wind" hypothesis,[11,16] whereby phonons emitted by droplets are reabsorbed in the droplet cloud, transferred momentum between droplets and effectively providing an expansive pressure to the cloud. Experimental evidence for this recombination phonon wind in Si has been provided by photoluminescence images of the cloud,[15] suggesting that screening plays a small role.

The ability of droplets to repel each other by a low-frequency phonon wind[16] is already sizeable at the pump-

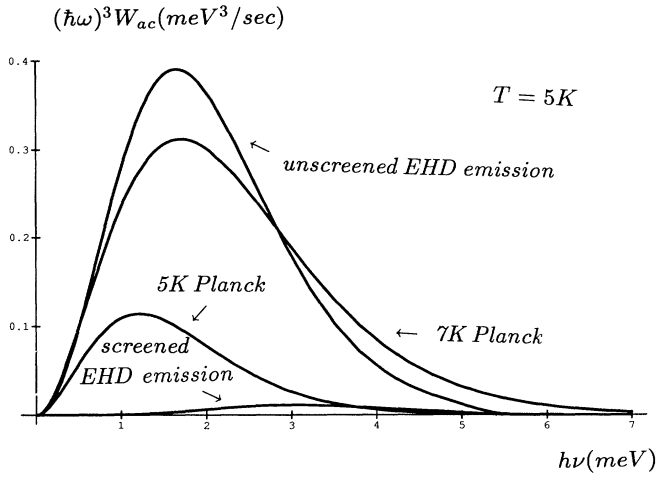

FIG. 6. Spectrum W_{ac} of low-frequency acoustic phonons emitted from EHD at 5 K (upper curve without high-frequency tail) in comparison to a pure Planck distribution (second curve from the top) at 7 and 5 K (third curve). We multiplied the spectra by the factor $(h\nu)^3$ to show the energy content. The lowest (fourth) curve is the droplet emission spectrum with screening taken into account.

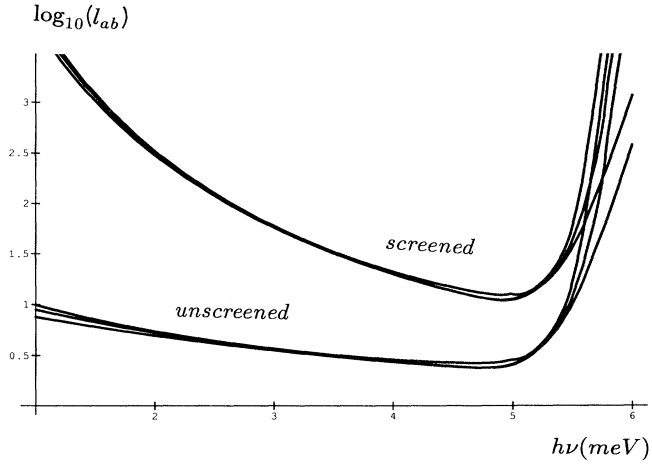

FIG. 7. Log_{10} of the mean free path l_{ab} (in cm) of low-frequency acoustic phonons as a function of their energy for different EHL temperatures (5, 7, 10 K from top to bottom for each family) with and without screening. The sharp rise in l_{ab} for phonons with frequencies above 5 meV is due to the $2k_F$ cutoff described in the text.

ing rate near the threshold discussed in Sec. II, because the absorption length in the liquid is about 3 μm without screening and the mean free path between droplets $1/\pi n_d R^2 \sim 1$ μm. The probability of being absorbed by one droplet is therefore 3–4 % implying that there are about 30 collisions before a phonon can leave the cloud. LA phonons play major role.

V. THE TEMPERATURE OF EHD

EHD experiments with steady-state pumping show that droplets may have a final temperature which is somewhat higher than that of the lattice. In particular, experimentally observed temperatures from photoluminescence spectra are found to be greater than about 5 K even at low lattice temperature.[13] Now we examine whether this effect can be attributed to an energy balance between Auger heating and carrier cooling by acoustic-phonon emission plus evaporation. The droplet heating process has direct consequences in the frequency distribution of emitted phonons.

Auger recombination in Si proceeds through *four*-particle collision with the fourth particle either a phonon or an extra carrier. We have seen in Fig. 4 that the initial energy of a hot carrier does not change Q_{cc} significantly and approximately 0.5 of the band-gap energy released in recombination returns to a 0.1-μm droplet (Sec. III). We assume equal input from electrons and holes, which turns out not to influence the results strongly. Using the Auger recombination time given above, we estimate the energy input per unit volume to be equal to

$$Q_{\text{Auger}} = nQ_{cc}/\tau_{\text{Auger}} , \tag{6.1}$$

given that in Eq. (4.5) the upper integration limit is ϵ_G, the semiconductor gap. On the basis of Eq. (5.1) the energy-loss power due to acoustic-phonon emission can be written as

$$Q_A = \frac{ms^2}{2k_e^3\tau_{Ae}} \left\{ \int_{m_e s}^{\infty} dk\, k f_e(\epsilon_k) \int_0^{2(k-m_e s)} dq\, q^3 S(q)(N_q+1)[1-f_e(\epsilon_k - sq)] \right.$$
$$\left. - \int_0^{\infty} dk\, k f_e(\epsilon_k) \int_0^{2(k+m_e s)} dq\, q^3 S(q) N_q [1-f_e(\epsilon_k + sq)] \right\} + Q_{A-h} , \tag{6.2}$$

where two integrals in the curly parentheses come from phonon emission and absorption, and the term Q_{A-h} represents the analogous expression for holes.

Another channel of relaxation exists due to surface evaporation of excitons (evaporation of single carriers is less probable).[8] We estimate this loss rate by using the conventional Richardson formula

$$Q_{\text{evap}} = \frac{3\nu_{\text{ex}} M_{\text{ex}} k_B^2 T^2}{4\pi^2 \hbar^3 R} e^{-\phi/k_B T} , \tag{6.3}$$

where $\nu_{\text{ex}}=24$, M_{ex}, ϕ are the excitonic reduced mass and binding potential. The dependence of $\log_{10}[(Q_A + Q_{\text{evap}})/Q_{\text{Auger}}]$ versus temperature is plotted in Fig. 8. The solution of the balance equation gives the steady-state temperature of EHD. We can see that the temperature $T=4$–7 K is obtained when the fraction of the initial energy transferred back to the droplet is 30–70 %, which is consistent with observations. At this temperature the influence of evaporation is small; the main channel of relaxation is due to phonons. If screening is taken into account, the temperature rises and, for instance, $T=8$–13 K results in the same range of input. The EHD luminescence spectra indicate a lower EHD temperature, so we conclude that screening should be neglected, in agreement with our previous estimates about the phonon wind. The same conclusion in this context was made earlier by Keldysh and Sibel'din.[11] If we assume an EHD heating of 5 K together with our balance calculation, then 55% of the initial hot-carrier energy should be retained in the droplet and the average droplet radius is surmised to be 0.1–0.12 μm depending upon the relative strength of the hole- and electron-assisted channels of Auger recombination in droplets.

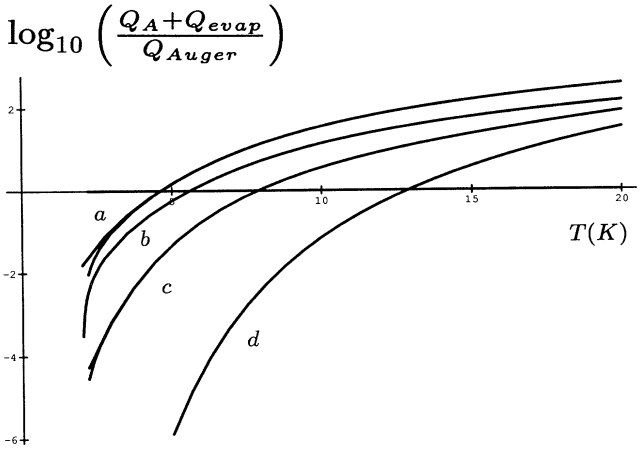

FIG. 8. The solution of the energy balance equation for the EHD temperature at a lattice temperature $T_L=2$ K. Curves from the top: (a) unscreened energy-loss rate when 30% of the Auger-released energy returns to the droplet. The branching at low temperatures accounts for pure spontaneous emission of phonons (upper branch) and spontaneous plus stimulated emission minus absorption [lower branch, $Q_A(T_L)=0$]; (b) unscreened energy-loss rate when 70% returns, all processes; (c) screened rate when 30% returns, branching has the same meaning; (d) evaporation energy loss only. The steady-state droplet temperature is each case is given by the point where the curve crosses the horizontal axis.

VI. CONCLUSION

In order to explain the observation of a localized source of low-frequency phonons produced by photoex-

cited Si, we have examined the possibility of replacing the phonon hot spot scenario by emission of phonons from electron-hole droplets. We have shown that intercarrier scattering effectively relaxes a good fraction of the hot-carrier energy within a droplet, bypassing the optical-phonon emission by hot carriers. The energy emitted by EHD is partly released by low-frequency acoustic phonons ($\nu \leq 0.75$ THz) which, we believe, contribute to the ballistic part of the heat pulse and the sharp caustics in the phonon images.[1,4] In effect, the droplets emit acoustic phonons with energy noticeably higher than that of lattice phonons because the droplet temperature does not relax to that of the surrounding lattice due to Auger heating and intercarrier relaxation. This implies that the localized phonon source is represented by the EHD cloud. This conclusion is supported by the observation that the phonon source lifetime is comparable—perhaps equal—to the measured EHD lifetime.

Further verification of this theory could be obtained from experimental measurements of the recombination luminescence performed in conjunction with heat-pulse experiments, or from comparitive experiments on other semiconductors such as GaAs or Ge in which the excitonic properties are quite different.

ACKNOWLEDGMENTS

M. E. M. and J. P. W. acknowledge discussions with J. A. Shields. M. E. M. and J. P. W. were supported by the NSF under the Material Research Laboratory Grant No. DMR-89-20538, and S. E. E. was supported by NSF-DMR-90-15791.

APPENDIX

We used the following parameters for Si:[8,19] the longitudinal velocity of sound, $s = 8.99 \times 10^5$ cm/s, the electric charge e; static dielectric permittivity, $\kappa = 11.7$; the effective electron density-of-states mass, $m_e = 0.3216m$, where m is the mass of a free electron; the density-of-states mass of holes, $m_h = 0.523m$; the electron Rydberg $E_e = m_e e^4/2\kappa^2\hbar^2 = 32.0$ meV; the hole Rydberg $E_h = m_h e^4/2\kappa^2\hbar^2 = 52.0$ meV; the EHD carrier concentration at zero temperature, $n = 3 \times 10^{18}$ cm^{-3}; the EHD binding energy, $\phi = 8.2$ meV; the optical-phonon energy, $\hbar\Omega_0 = 63.34$ meV; and the reference wave vector of an electron having energy equal to $\hbar\Omega_0$, $k_e = 7.312 \times 10^6$ cm^{-1}. The same wave vector for a hole is $k_h = 9.32 \times 10^6$ cm^{-1}.

In treating the energy-loss rate of hot electrons we followed Refs. 10 and 18. We included the weak logarithmic dependence into the nominal times. The nominal $\alpha\beta$ scattering time is

$$\frac{1}{\bar{\tau}_{\alpha\beta}} = \frac{16\pi n E_\beta}{\hbar k_\beta^3} \left[\frac{m_\alpha}{m_\beta} \right]^{1/2} \ln \left[\frac{\zeta \epsilon^{3/2}}{\hbar\omega_\beta E_\beta^{1/2}} \left[\frac{m_\beta}{m_\alpha} \right]^{3/2} \right] . \tag{A1}$$

Here α,β denote subscripts e and/or h, $\zeta = 2.246$,[18] $\hbar\omega_{e,h} = \sqrt{4\pi n e^2/\kappa m_{e,h}}$ are plasma frequencies for electrons and holes (not to be confused with plasmon modes for the entire droplet), which equal 33 and 26 meV, respectively.

The nominal time of an optical-phonon emission by holes due to deformation-potential coupling, $\bar{\tau}_{Oh} = 0.5 \times 10^{-12}$ s. The corresponding time for electrons is not known to us, so we assume the *same* value for $\bar{\tau}_{Oe}$. The nominal time of an acoustic-phonon emission by a carrier due to the deformation potential, $\bar{\tau}_{Ae} = 0.2 \times 10^{-12}$ s, $\bar{\tau}_{Ah} = 1.2 \times 10^{-12}$ s.

[1] J. A. Shields, M. Msall, M. Carroll, and J. P. Wolfe, Phys. Rev. B **47**, 12 510 (1993).
[2] D. V. Kazakovtsev and Y. B. Levinson, Zh. Eksp. Teor. Fiz. **88**, 2228 (1985) [Sov. Phys. JETP **61**, 1318 (1985)]; Phys. Status Solidi **136**, 425 (1986).
[3] J. C. Hensel and R. C. Dynes, Phys. Rev. Lett. **39**, 969 (1977).
[4] J. A. Shields and J. P. Wolfe, Z. Phys. B **75**, 11 (1989).
[5] W. E. Bron, in *Nonequilibrium Phonons in Nonmetallic Crystals,* Vol. 16 of *Modern Problems in Condensed Matter Sciences,* edited by W. Eisenmenger and A. A. Kaplyanskii (North-Holland, Amsterdam, 1986).
[6] S. Tamura, Phys. Rev. B **27**, 858 (1983).
[7] S. Tamura, Phys. Rev. B **31**, 2574 (1985).
[8] T. M. Rice, J. C. Hensel, T. G. Phillips, and G. A. Thomas, in *Electron-Hole Liquid in Semiconductors,* edited by H. Ehrenreich, F. Seitz, and D. Turnbull, Solid State Physics Vol. 32 (Academic, New York, 1977).
[9] J. P. Wolfe, J. Lumin. **30**, 82 (1985).
[10] S. E. Esipov and Y. B. Levinson, Adv. Phys. **36**, 331 (1987).
[11] L. V. Keldysh and N. N. Sibel'din, in *Nonequilibrium Phonons in Nonmetallic Crystals* (Ref. 5).
[12] F. M. Steranka and J. P. Wolfe, Phys. Rev. B **34**, 1014 (1986).
[13] P. L. Gourley and J. P. Wolfe, Phys. Rev. B **24**, 5970 (1981).
[14] H. Yoshida, H. Saito, and S. Shionoya, Phys. Status Solidi B **104**, 331 (1981).
[15] M. A. Tamor and J. P. Wolfe, Phys. Rev. B **26**, 5743 (1982).
[16] L. V. Keldysh, Pis'ma Zh. Eksp. Teor. Fiz. **23**, 100 (1976) [JETP Lett. **23**, 86 (1976)].
[17] W. Dietsche, S. J. Kirch, and J. P. Wolfe, Phys. Rev. B **26**, 780 (1982).
[18] H. Kramers, Physica **13**, 401 (1947); D. Pines, Phys. Rev. **85**, 931 (1952).
[19] V. F. Gantmakher and Y. B. Levinson, *Carrier Scattering in Metals and Semiconductors* (North-Holland, Amsterdam, 1987).